

Theoretical and Experimental Analysis of the Integrating Luminous Fluxmeter Systems

Dragan D. Vučković and Predrag D. Rančić
University of Niš, Faculty of Electronic Eng., Lab. of E.I. & I.E.,
18000 Niš, Beogradska 14, Srbija
dvucko@elfak.ni.ac.yu, prancic@elfak.ni.ac.yu

Abstract – Theoretical and experimental analysis of the luminous flux distribution inside the closed space illuminated by an electrical light source (ELS) of unknown total luminous flux is presented in this paper. Presented results suggest that beside the commonly used Ulbricht's sphere several different closed spaces with precious geometries can be used for total luminous flux measurement (i.e., as the integrating closed space – ICS). The mathematical model used in analysis is based on the luminous flux conservation law, expressed through System of the Interreflection Equations of the Luminous Flux (SIE-LF, [1]-[6]). More precisely, the three-surface model of the ICS with ideally diffuse (Lambertian) characteristics of the three interior surfaces is used in analysis.

The SIE-LF is applied on the following geometries of the ICS:

- Sphere (so called Ulbricht's sphere);
- Parallelepiped with square bases; and
- Cylinder with circular bases, or bases that are spherical sectors of the circumscribed sphere. ([6]-[8]).

Results of the SIE-LF are obtained in the form convenient for further analyses and optimization of the ICS geometry. A number of numerical experiments were performed in cases when the ICS are illuminated by the ELSs with known Luminous Intensity Distribution Function (LIDF). This included: the "pear shaped" ELSs (standard bulb lamps) and ELSs in the shape of thin lengthened cylinder (fluorescent tubes). These experiments illustrate possibilities of using the alternative geometries for luminous flux measurement, as well as the estimation of the part of the error obtained in measurement.

The Integrating Luminous Fluxmeter System (ILFS) is realized in the Laboratory of Electrical Installations and Illumination Engineering (Lab. of E.I.&I.E.) at the University of Nis, Faculty of Electronic Engineering, based on the previous theoretical analysis of the ICS cube geometry. That system consists of:

- The cube shaped ICS;
- The LMT Digital Illuminance Meter B510 with Photometer Head P 30 SC0 placed in the center of one cube surface, used for the measurement of the indirect illuminance component;
- The ELS with unknown luminous flux, placed in the cube center;
- The stabilized power supply, as well as the equipment for voltage and current control (measurement);
- The circular screen (baffle) placed between the ELS and photometer head; and
- The *OSRAM* etalons (standards) ELSs.

The main part of previous experimental and related theoretical results is given in [9] and [10]. Some of these results are used in this paper for more general analysis. This analysis indicates that the place and the size of the screen are not critical what in turn allows the wide range for the selection of the screen place and size.

Key words: *Integrating Luminous Fluxmeter Systems, Integrating Closed Space, Luminous Flux, Indirect Illuminance, Electrical Light Source, System of the Interreflection Equations of the Luminous Flux, Methodical Error.*

1. INTRODUCTION

Measurement of the ELS' luminous flux is very important process in the lighting characterization of the ELS (and the luminaires), in the design and development of the ELSs, as well as in the quality control during the ELS production and in assembling of the ELS' catalogue materials. A lot of references consider the theoretical and experimental aspects of this problem, what indicates its significance. Authors are not going to present detailed bibliography of this research area, except of pointing to references [2], [3], [5], [6] and [11], where can be found the review and detailed bibliography.

Two methods are mostly used for the ELS' luminous flux measurement until now:

- The integrating fluxmeter method (IFM); and
- The goniophotometer method (GPM).

First method can be characterized as the direct method for the luminous flux measurement, i.e., the luminous flux is directly proportional to the indirect illuminance component at the measuring point of the ICS, which is illuminated by the ELS of unknown luminous flux. The closed space sphere shaped (Ulbricht's sphere) which interior surface is uniformly painted with white color of ideally diffuse characteristics (Lambertian surface) is mostly used for that purpose. Indirect illuminance of the arbitrary point at the interior sphere surface, for arbitrary position of the light source, is constant and proportional to the total radiated luminous flux of the ELS. Thus, the sphere is optimal ICS and it is necessary to have the radius as large as possible in order that, during the measurement, ELS would represent the point light source as well as would require relatively small screen. The usage of a small screen minimally perturbs the light field inside the sphere, and in that way, its optimization and proper location can minimize methodical error.

Second method corresponds to the indirect measurement of the luminous flux, i.e., the first step is recording of the ELS' luminous intensity spatial distribution, and after that radiated luminous flux is calculated based on the general (integrating) definition expression.

Both methods are currently used for measurements. The ILFS is mostly used for luminous flux measurement, while the second method is used for the measurement of the spatial luminous intensity distribution of luminaires, which is necessary characteristic for the interior and exterior lighting design. Datum of the luminaire's total luminous flux, which is then obtaining by the calculation, enables the determination of the luminaire's luminous flux utilization coefficient, if the luminous flux of the built-in light sources is known (CIE code flux number $N_s = \eta_{sv}$).

Due to the difficulties that authors had during the construction of the mechanical part of the measuring systems (sphere and mechanical construction of the goniophotometer), in the Lab. of E.I. & I.E., it was started with theoretical analysis with the aim to use some other ICSs with precious geometry and easier for construction, instead of the sphere geometry. One part of these theoretical and experimental researches is presented in this paper.

This paper consists two parts.

The used SIE-LF method as well as the analysis of the luminous flux distribution solutions on the sphere, parallelepiped and cylinder surfaces are presented in the first part. Analysis is aimed on the research of the possibilities for using of the parallelepiped shaped ICS with square bassettes as well as the cylinder shaped ICS with circular bassettes (or with spherical sector bassettes) in the ILFS. The geometry of the ICS is particularly analyzed in the aim of the mathematical model methodical error minimization.

In the second part of the paper, some numerical experiments are given first, which for the adopted mathematical models of ICSs, illustrate possibilities of their usage in cases when the ICSs are illuminated by pear shaped ELS or by the ELS in the shape of thin lengthened cylinder (standard bulb lamps and fluorescent tubes). Summary of the results related to the realized ILFS', with the cube as the ICS, is also presented in this part of the paper.

2. THE THEORETICAL BACKGROUND

2.1. General Expression of the SIE-LF

A closed space whose interior is illuminated by the ELS is considered. All interior N surfaces are ideally diffuse (Lambertian) with known reflectances ρ_i , $i=1, 2, \dots, N$. Total surface of the closed space is $S = S_1 + S_2 + \dots + S_N$. Number N describes so called N -surface

model of the ICS. The ELS location as well as its Luminous Intensity Distribution Function (LIDF), $I(\hat{r}_k) = I(\gamma, \varphi)$ in [cd], are known. Direct component of the luminous flux on individual k -th surface, Φ_{0k} , $k=1, 2, \dots, N$, $\Phi_0 = \Phi_{01} + \Phi_{02} + \dots + \Phi_{0N}$, is determined on the basis of the definition expression:

$$\Phi_{0k} = \int_{\Omega_k} I(\hat{r}_k) d\Omega_k = \int_{S_k} I(\hat{r}_k) \frac{d\vec{S}_k \cdot \hat{r}_k}{r_k^2}, \quad k=1, 2, \dots, N, \quad (1)$$

where: Ω_k - the solid angle subtended by the k -th surface of the closed space as seen from the ELS, and \hat{r}_k - the ort vector.

The SIE-LF, which expresses the law of luminous flux conservation, in the case of the closed space is

$$\Phi_{0k} = \sum_{i=1}^N (\delta_{ik} - \rho_i f_{i,k}) \Phi_i, \quad k=1, 2, \dots, N, \quad (2)$$

where: δ_{ik} - Kronecker symbol, $\Phi_i = \Phi_{0i} + \Phi_{ind i}$ - the total luminous flux on the i -th surface (Φ_{0i} - direct and $\Phi_{ind i}$ - indirect component), $f_{i,k}$ - the form factor (coefficient of interreflection) given by the double surface Fredholm's integral

$$f_{i,k} = \frac{1}{S_i} \iint_{S_i S_k} \frac{\cos \gamma_i \cdot \cos \gamma_k}{\pi r_{ik}^2} dS_i dS_k, \quad i, k=1, 2, \dots, N. \quad (3a)$$

General relations are always valid for the form factors, for each closed space consisted of N ideally diffuse surfaces

$$S_i f_{i,k} = S_k f_{k,i}, \quad i, k=1, 2, \dots, N, \quad (3b)$$

$$\sum_{k=1}^N f_{i,k} = 1, \quad i=1, 2, \dots, N, \quad (3c)$$

where (3b) expresses the reciprocity law, and (3c) is also the law of luminous flux conservation consequence. The form factors ($f_{i,k}$) can be determined using (3a-c), and its substitution into (2) leads to the solution of the SIE-LF. The luminous flux distribution of the closed space surfaces as well as the average values of the plane illuminance of these surfaces is obtained on that way. The mean direct component of plane illuminance is

$$E_{0k} = \Phi_{0k} / S_k, \quad i, k=1, 2, \dots, N, \quad (4a)$$

and the mean indirect component of the plane illuminance is

$$E_{ind k} = \Phi_{ind k} / S_k, \quad i, k=1, 2, \dots, N. \quad (4b)$$

- In the following considerations, in front of the existing indexes following ones will be added: s – in the sphere case, p – in the parallelepiped case, and c – in the cylinder case, e.g.: $\Phi_{ind sk}$ - denotes the indirect luminous flux on the k -th surface of the integrating sphere, $f_{pi, pk}$ - denotes the form factor between the i -th and the k -th surfaces of the parallelepiped, $E_{ind ck}$ - denotes mean indirect illuminance of the k -th cylinder surface, etc.
- Three-surfaced model ($N=3$) will be considered in all three cases, while the all three parts of the Lambertian surface are with the same reflectance coefficients $\rho_1 = \rho_2 = \rho_3 = \rho$.
- For the determination of the direct luminous fluxes Φ_{0k} , $k=1, 2, 3$ according to (1), two types of the ELSs are considered, for the purpose in further theoretical analysis:

- Type A - pear shaped ELS (standard bulb lamp) whose LIDF is given by the following expression

$$I(\hat{r}) = I(\gamma, \varphi) = 0.5 I_0 (1 + \cos \gamma), \quad \gamma \in [0, \pi]; \quad (5a)$$

- Type B - ELS in the shape of thin lengthened cylinder (fluorescent tube) whose LIDF is given by the following expression

$$I(\hat{r}) = I(\gamma, \varphi) = I_0 \sin \gamma, \quad \gamma \in [0, \pi]. \quad (5b)$$

2.2. The Integrating Sphere

Form factors in the case of the sphere shaped ICS with radius R_s and Lambertian arbitrary painted interior surfaces have simple solutions ([7])

$$f_{si, sk} = S_{sk} / S_s, \quad i, k = 1, 2, \dots, N, \quad (6)$$

and the analytical solutions for (2) can be obtained easily ([6] i [7]). Indirect illuminance component of any point at the sphere surface, in the case of the uniformly painted sphere surface $\rho_{si} = \rho_s$, $i = 1, 2, \dots, N$, Fig. 1, using the solutions of the SIE-LF (2), has the known simple uniform solution, given by expression

$$E_{ind sk} = \frac{\Phi_{ind sk}}{S_{sk}} = \frac{\sum_{i=1}^N \rho_{si} \Phi_{0si}}{S_s [1 - (\sum \rho_{si} S_{si}) / S_s]} = \frac{\rho_s}{S_s (1 - \rho_s)} \Phi_{0s} = C_s \Phi_{0s}, \quad k = 1, 2, \dots, N, \quad (7)$$

i.e. the indirect illuminance is directly proportional to the ELS' totally radiated (direct) luminous flux in any point P at the uniformly painted sphere surface.

For the measurement of the indirect illuminance, it is necessary, according to Fig. 1, to place the screen Z . The screen Z should be placed in the way that its size and place minimally perturbs light field and in that way minimally disturbs the direct proportionality (7), i.e. includes the minimal methodical screen error. Relating to the mathematical model, the methodical measuring error of the real model is influenced by accuracy of the sphere surface construction and the accuracy of the used illuminance meter, as well as the accuracy of the method for the integrating sphere factor C_s determination.

2.3. The Integrating Parallelepiped

The parallelepiped shaped ICS as a three-surface model has square bases of the side a , surfaces $S_{p1} = S_{p3} = a^2$, and lateral surfaces of the length H_p and of the area $S_{p2} = 4 a H_p$, Fig. 2. Interior surface is uniformly painted so it holds: $\rho_{p1} = \rho_{p2} = \rho_{p3} = \rho_p$.

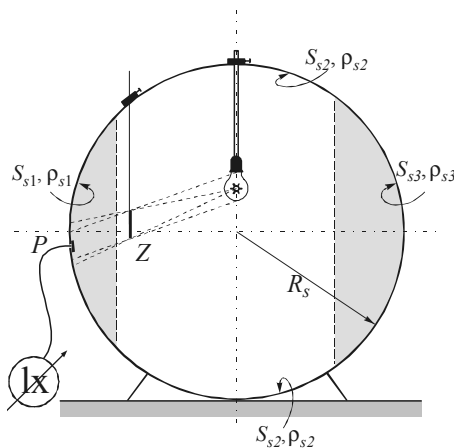


Fig. 1: The mathematical model of the sphere ICS.

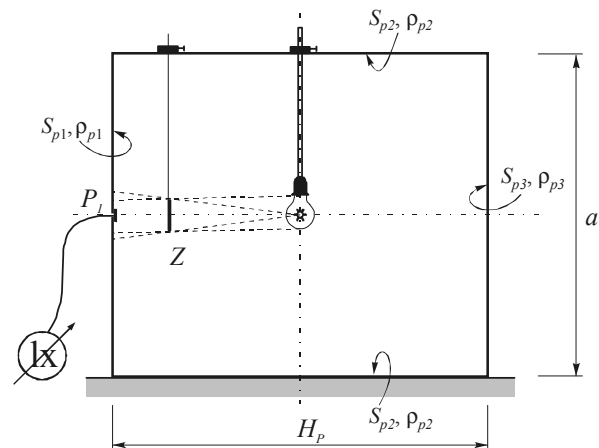


Fig. 2: The mathematical model of the parallelepiped ICS.

Form factors in the case of this geometry and in case of $A_p = a / H_p$ are:

- according to (3a)

$$f_{p1,p1} = f_{p3,p3} = 0, \quad (8a)$$

$$F_p = f_{p1,p3} = f_{p3,p1} = \frac{4}{\pi A_p} \left[\sqrt{1 + A_p^2} \arctg \frac{A_p}{\sqrt{1 + A_p^2}} - A_p \arctg A_p + \frac{1}{4 A_p} \ln \frac{(1 + A_p^2)^2}{(1 + 2 A_p^2)} \right]; \quad (8b)$$

- and according to (3b) and (3c) follows

$$f_{p1,p2} = 1 - f_{p1,p3} = 1 - F_p, \quad (8c)$$

$$f_p = f_{p2,p1} = f_{p2,p3} = \frac{S_{p1}}{S_{p2}} (1 - F_p) = \frac{A_p}{4} (1 - F_p), \quad (8d)$$

$$f_{p2,p2} = 1 - 2 f_{p2,p1} = 1 - 2 f_p. \quad (8e)$$

After solving of the SIE-LF (2) by the variable eliminating method, the following is obtained

$$\Phi_{p1} = C \frac{1 + C(F_p / f_p - 1)}{1 - C^2(F_p / f_p - 1)^2} \frac{\Phi_{0p}}{1 - \rho_p} + (1 - C) \frac{\Phi_{0p1} + C(F_p / f_p - 1)\Phi_{0p3}}{1 - C^2(F_p / f_p - 1)^2}, \quad (9a)$$

$$\Phi_{p3} = C \frac{1 + C(F_p / f_p - 1)}{1 - C^2(F_p / f_p - 1)^2} \frac{\Phi_{0p}}{1 - \rho_p} + (1 - C) \frac{\Phi_{0p3} + C(F_p / f_p - 1)\Phi_{0p1}}{1 - C^2(F_p / f_p - 1)^2}, \quad (9b)$$

$$\Phi_{p2} = \left[1 - \frac{2C}{1 - C(F_p / f_p - 1)} - \frac{(1 - C)(1 - \rho_p)}{1 - C(F_p / f_p - 1)} \right] \frac{\Phi_{0p}}{1 - \rho_p} + (1 - C) \frac{\Phi_{0p2}}{1 - C(F_p / f_p - 1)}, \quad (9c)$$

where: C - the new constant, $C = \rho_p f_p / (1 + \rho_p f_p)$, Φ_{0p} - the total direct flux $\Phi_{0p} = \Phi_{0p1} + \Phi_{0p2} + \Phi_{0p3}$, i.e. total unknown ELS' luminous flux.

Simple analysis of (9a) shows that influence of the unknown direct flux Φ_{0p3} on the solution for the total luminous flux on the base of area S_{p1} , can be eliminated by adopting the ratio $F_p / f_p = 1$. This ratio corresponds to the approximately cube geometry, i.e. $A_p = a / H_p \cong 1$. Solutions for the (9a-c) now obtain simpler forms:

$$\Phi_{p1} = \Phi_{0p1} + \Phi_{ind p1} = C \frac{\Phi_{0p}}{1 - \rho_p} + (1 - C) \Phi_{0p1}, \quad (10a)$$

$$\Phi_{p3} = \Phi_{0p3} + \Phi_{ind p3} = C \frac{\Phi_{0p}}{1 - \rho_p} + (1 - C) \Phi_{0p3}, \quad (10b)$$

$$\Phi_{p2} = \Phi_{0p2} + \Phi_{ind p2} = [1 - 2C - (1 - C)(1 - \rho_p)] \frac{\Phi_{0p}}{1 - \rho_p} + (1 - C) \Phi_{0p2}, \quad (10c)$$

and the mean indirect illuminance of the base of area S_{p1} is

$$E_{ind p1} = \frac{\Phi_{ind p1}}{S_{p1}} = \frac{C}{S_{p1}} \frac{\Phi_{0p}}{1 - \rho_p} - \frac{C}{S_{p1}} \Phi_{0p1}. \quad (11)$$

Last expression indicates the possibilities of the ELSs luminous flux measurement.

The indirect illuminance of the point P_1 vicinity, i.e. the indirect illuminance which is measured at the point P_1 , has also to be theoretically determined first in order to explicitly prove the previous claim. The illuminance of the point P_1 vicinity, placed in the center of the surface S_{p1} , can be determined by the solutions (10a-c) and solutions from [11].

Luminous exitances of surfaces S_{p2} and S_{p3} are: $M_{p2} = \rho_p \Phi_{p2} / S_{p2} = \pi L_{p2}$ and $M_{p3} = \rho_p \Phi_{p3} / S_{p3} = \pi L_{p3}$, where L_{p2} and L_{p3} are equivalent resulting luminances of the surfaces 2 and 3 which have Lambertian characteristics. Indirect illuminance of the point P_1 vicinity is:

$$E_{ind\ p\ P1} = M_{p2} + (M_{p3} - M_{p2})C_1 = \frac{\rho_p(1-C_1)}{4S_{p1}}[\Phi_{p2} + \frac{4C_1/A_p}{1-C_1}\Phi_{p3}] \quad (12a)$$

where C_1 is constant, given by the expression: $C_1 = \frac{4}{\pi} \frac{A_p}{\sqrt{4+A_p^2}} \arctg \frac{A_p}{\sqrt{4+A_p^2}}$.

Indirect illuminance of the point P_1 vicinity, for $F_p/f_p = 1$ and using the luminous flux distribution solutions (10a-c), i.e. for $A_p = a/H_p \cong 1$, $f_p = 0.2$, $\Phi_{0p1} \cong \Phi_{0p3}$, and $C_1 = \frac{4}{\pi} \frac{1}{\sqrt{5}} \arctg \frac{1}{\sqrt{5}} = 0.2395$, can be expressed by the following expression

$$E_{ind\ p\ P1} = C_p (1 + \varepsilon_p) \Phi_{0p}, \quad (12b)$$

where: C_p - the integrating parallelepiped (cube) factor calculated for $A_p = 1$,

$$C_p = \frac{\rho_p(1-C_1)(1+2\frac{3C_1-1}{1-C_1}C)}{4S_{p1}(1-\rho_p)} = \frac{0.19}{S_{p1}} \frac{\rho_p}{1-\rho_p} \frac{5+0.26\rho_p}{5+\rho_p}, \quad (13)$$

and $\varepsilon_p = \varepsilon_{p1} \cdot \varepsilon_{p2}$, ε_{p1} - is the methodical error caused by the proposed parallelepiped (cube) model, and ε_{p2} - is the error caused by the ESI' luminous flux distribution, i.e.:

$$\varepsilon_{p1} = \frac{(1-C)(1-\rho_p)}{1+(2\frac{3C_1-1}{1-C_1})C} (2\frac{3C_1-1}{1-C_1}) = -0.74 \frac{5(1-\rho_p)}{5+0.26\rho_p}, \quad (14a)$$

$$\varepsilon_{p2} = \Phi_{0p1} / \Phi_{0p}, \quad (14b)$$

The error caused by the screen is not enlaced by this expression.

2.4. The Integrating Cylinder

The cylinder shaped ICS as a three-surface model has circular bases of the radius R_c , of area $S_{c1} = S_{c3} = \pi R_c^2$, and shell of the length H_c and of the area $S_{c2} = 2\pi R_c H_c$, Fig. 3. Interior surface is uniformly painted so it holds: $\rho_{c1} = \rho_{c2} = \rho_{c3} = \rho_c$.

Form factors for cylinder shaped ICS are:

- according to (3a)

$$f_{c1,c1} = f_{c3,c3} = 0, \quad (15a)$$

- and according to (3b), (3c), (6), using the method of the equivalent sphere ([7] and [8]), Fig. 4, follows

$$f_{ci,ck} = \frac{S_{si}}{S_{ci}} \frac{S_{sk}}{S_s}, \quad i, k = 1, 2, 3, \quad i \neq k. \quad (15b)$$

If by F_c is denoted the following form factor: $F_c = f_{c1,c3} = f_{c3,c1}$, and by f_c is denoted the following form factor: $f_c = f_{c2,c1}$, solutions for the distribution of the luminous flux are obtained in the same form as in (9a-c), i.e.:

$$\Phi_{c1} = C \frac{1 + C(F_c/f_c - 1)}{1 - C^2(F_c/f_c - 1)^2} \frac{\Phi_{0c}}{1 - \rho_c} + (1 - C) \frac{\Phi_{0c1} + C(F_c/f_c - 1)\Phi_{0c3}}{1 - C^2(F_c/f_c - 1)^2}, \quad (16a)$$

$$\Phi_{c3} = C \frac{1 + C(F_c/f_c - 1)}{1 - C^2(F_c/f_c - 1)^2} \frac{\Phi_{0c}}{1 - \rho_c} + (1 - C) \frac{\Phi_{0c3} + C(F_c/f_c - 1)\Phi_{0c1}}{1 - C^2(F_c/f_c - 1)^2}, \quad (16b)$$

$$\Phi_{c_2} = \left[1 - \frac{2C}{1 - C(F_c/f_c - 1)} - \frac{(1 - C)(1 - \rho_c)}{1 - C(F_c/f_c - 1)} \right] \frac{\Phi_{0c}}{1 - \rho_c} + (1 - C) \frac{\Phi_{0c2}}{1 - C(F_c/f_c - 1)}, \quad (16c)$$

where: $C = \rho_c f_c / (1 + \rho_c f_c)$ and Φ_{0c} , $\Phi_{0c} = \Phi_{0c1} + \Phi_{0c2} + \Phi_{0c3}$ - is the total unknown (direct) luminous flux of ELS. After eliminating the influence of the Φ_{0c3} in the solution (16a), by adopting $F_c = f_c$, i.e. $A_c = 2R_c / H_c = 4/3$, the following is obtained:

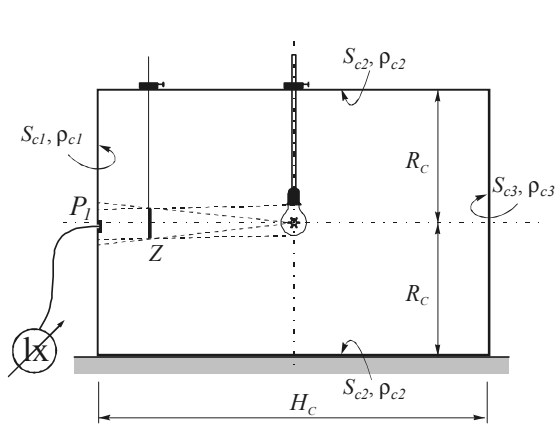


Fig. 3: The mathematical model of the cylinder for measurement of the luminous flux of the ELS Type A.

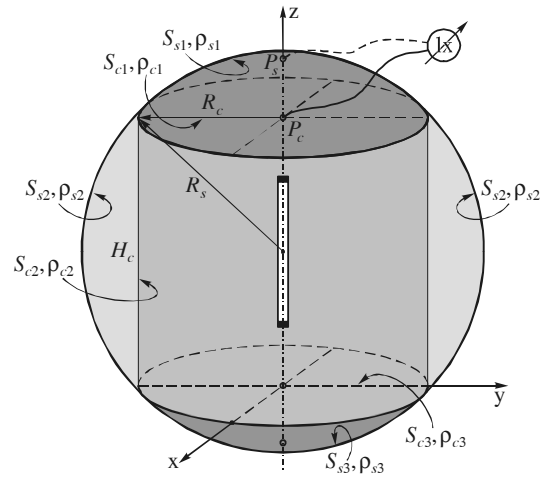


Fig. 4: The mathematical model of cylinder shaped ICS and the equivalent circumscribed sphere.

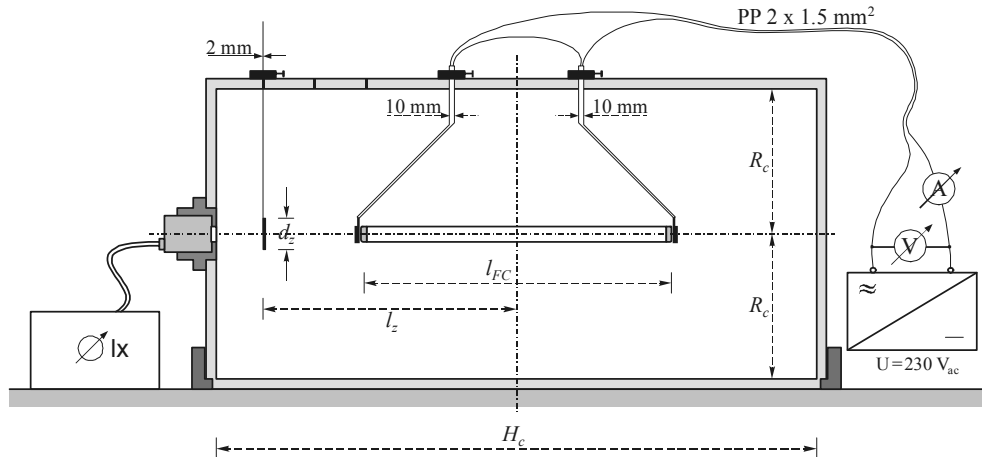


Fig. 5: The mathematical model of the cylinder shaped ICS for the ELS Type B luminous flux measurement. Screen Z is not necessary in this case.

$$\Phi_{c1} = \Phi_{0c1} + \Phi_{indc1} = C \frac{\Phi_{0c}}{1 - \rho_c} + (1 - C) \Phi_{0c1}, \quad (17a)$$

$$\Phi_{c3} = \Phi_{0c3} + \Phi_{indc3} = C \frac{\Phi_{0c}}{1 - \rho_c} + (1 - C) \Phi_{0c3}, \quad (17b)$$

$$\Phi_{c2} = \Phi_{0c2} + \Phi_{indc2} = [1 - 2C - (1 - C)(1 - \rho_c)] \frac{\Phi_{0c}}{1 - \rho_c} + (1 - C) \Phi_{0c2}, \quad (17c)$$

and the mean indirect illuminance of the base of area S_{c1} is:

$$E_{indc1} = \frac{\Phi_{indc1}}{S_{c1}} = \frac{C}{S_{c1}} \frac{\Phi_{0c}}{1 - \rho_c} - \frac{C}{S_{c1}} \Phi_{0c1}. \quad (18)$$

The indirect illuminance of the point P_1 vicinity, where the measurement is performed, i.e. in the center of the base of area S_{c1} , is

$$E_{indcP_1} = M_{c2} + (M_{c3} - M_{c2}) \frac{R_c^2}{R_c^2 + H_c^2} = \frac{\rho_c H_c}{2\pi R_c (R_c^2 + H_c^2)} (\Phi_{c2} + 2 \frac{R_c}{H_c} \Phi_{c3}), \quad (19a)$$

where: $M_{c2} = \rho_c \Phi_{c2} / S_{c2} = \pi L_{c2}$ and $M_{c3} = \rho_c \Phi_{c3} / S_{c3} = \pi L_{c3}$ - are luminous exitances of the surfaces (S_{c2} and S_{c3}), and L_{c2} and L_{c3} - are equivalent resulting luminances of the surfaces (S_{c2} and S_{c3}) with Lambertian characteristics.

In the case of $F_c = f_c$, which leads to $A_c = 4/3$ and $f_c = 0.25$, and with the assumption that $\Phi_{0c1} \cong \Phi_{0c3}$, indirect illuminance of the point P_1 vicinity is:

$$E_{indcP_1} = C_c (1 + \epsilon_c) \Phi_{0c}, \quad (19b)$$

where: C_c - integrating cylinder factor calculated for $A_c = 4/3$,

$$C_c = \frac{9(3 - 2C)}{52\pi H_c^2} \frac{\rho_c}{1 - \rho_c} = \frac{0.07}{S_{c1}} \frac{\rho_c}{1 - \rho_c} \frac{12 + \rho_c}{4 + \rho_c}, \quad (20)$$

and $\epsilon_c = \epsilon_{c1} \cdot \epsilon_{c2}$, ϵ_{c1} - methodical error caused by the adopted geometry of cylinder, ϵ_{c2} - error caused by the ESI luminous flux distribution, i.e.

$$\epsilon_{c1} = -2 \frac{(1 - C)(1 - \rho_c)}{3 - 2C} = -\frac{8(1 - \rho_c)}{12 + \rho_c}, \quad (21a)$$

$$\epsilon_{c2} = \Phi_{0c1} / \Phi_{0c}. \quad (21b)$$

The error caused by the screen is not enlaced by this expression.

Solutions for the cylinder with bases of circumscribed spherical sectors, *Fig. 4*, are not considered in this paper.

3. EXPERIMENTS

3.1. Numerical experiments

The methodical error for ICS in the shape of the parallelepiped (cube) and the cylinder is numerically estimated for the two cases of the ELSs (bulb lamp and fluorescent tube) that can be approximately determined for the LIDF (expressions (5a) and (5b)), in order to illustrate the validity of the proposed solutions.

Methodical errors of the proposed mathematical measuring models, for adopted geometries of the parallelepiped $A_p = a / H_p \cong 1$ and the cylinder $A_c = 2R_c / H_c = 4/3$, are given by expressions (14a) and (21a), respectively, i.e.:

$$\epsilon_{p1} = -\frac{3.7}{5 + 0.26\rho_p}(1 - \rho_p), \quad (22a)$$

$$\epsilon_{c1} = -\frac{8}{12 + \rho_c}(1 - \rho_c). \quad (22b)$$

3.1.1 ELS in the shape of the pear (Type A – Standard bulb lamp)

Errors that are results of the luminous flux distribution of the Type A ELSs for the parallelepiped (cube) and cylinder respectively are:

$$\epsilon_{p2A} = \frac{\Phi_{0p1}}{\Phi_{0p}} = \frac{1}{4} \left(1 - \frac{2}{\pi} \arctg \frac{1}{\sqrt{1 + 2A_p^2}} \right) = 0.1667 \quad (23a)$$

$$\epsilon_{c2A} = \frac{\Phi_{0c1}}{\Phi_{0c}} \cong \frac{1}{\pi} \frac{A_c}{\sqrt{1 + A_c^2}} \arctg A_c = 0.2361 \quad (23b)$$

Total errors with reflectance as a parameter are:

$$\boxed{\epsilon_{pA} = |\epsilon_{p1}| \epsilon_{p2A} = \frac{0.6167}{5 + 0.26\rho_p}(1 - \rho_p),} \quad (24a)$$

$$\boxed{\epsilon_{cA} = |\epsilon_{c1}| \epsilon_{c2A} = \frac{1.8890}{12 + \rho_c}(1 - \rho_c).} \quad (24b)$$

Numerical results of errors are shown on Fig. 6a with reflectance as a parameter.

3.1.2 The ELS in the shape of thin lengthened cylinder (Type B - Fluorescent tube)

Errors that are results of the luminous flux distribution of the Type B ELS for the parallelepiped (cube) and the cylinder respectively are:

$$\epsilon_{p2B} = \frac{\Phi_{0p1}}{\Phi_{0p}} \cong \frac{1}{\pi} \left(\arctg \frac{2A_p}{\sqrt{\pi}} - \frac{2\sqrt{\pi}A_p}{\pi + 4A_p^2} \right) = 0.1112, \quad (25a)$$

$$\epsilon_{c2B} = \frac{\Phi_{0c1}}{\Phi_{0c}} = \frac{1}{\pi} \left(\arctg A_c - \frac{A_c}{A_c^2 + 1} \right) = 0.1424. \quad (25b)$$

Total errors with reflectance as a parameter are:

$$\boxed{\epsilon_{pB} = |\epsilon_{p1}| \epsilon_{p2B} = \frac{0.4114}{5 + 0.26\rho_p}(1 - \rho_p),} \quad (26a)$$

$$\boxed{\epsilon_{cB} = |\epsilon_{c1}| \epsilon_{c2B} = \frac{1.1392}{12 + \rho_c}(1 - \rho_c).} \quad (26b)$$

Numerical results of errors are shown on Fig. 6b with reflectance as a parameter.

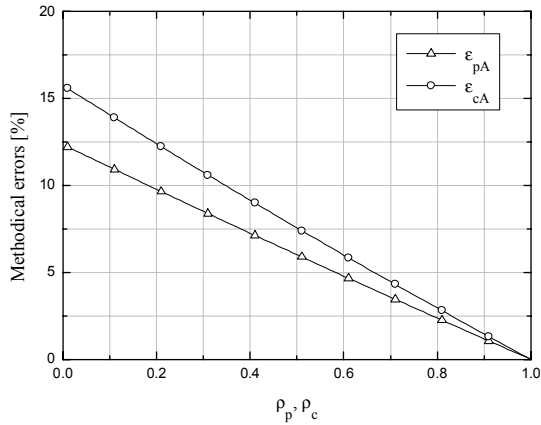


Fig. 6a Methodical errors caused by the geometry of ICS in the shape of parallelepiped (cube) and cylinder as well as luminous flux distribution of the Type A, with reflectance as a parameter

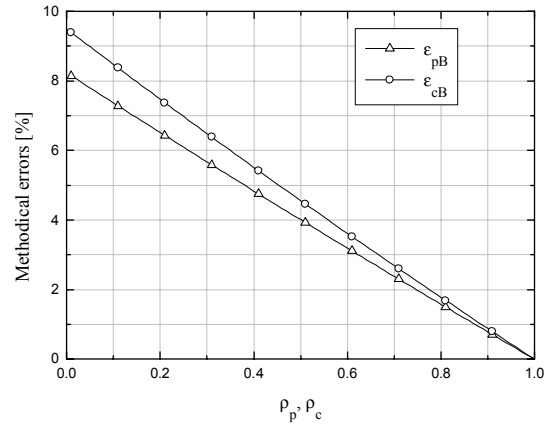


Fig. 6b Methodical errors caused by the geometry of ICS in the shape of parallelepiped (cube) and cylinder as well as luminous flux distribution of the Type B, with reflectance as a parameter

3.2. Experimental results related to the developed ILFS Laboratory model

The ILFS Laboratory model constructed in the Lab. of E.I. & I.E. is given schematically in the Fig. 7a and its photography is given in Fig. 7b. It was assumed that indirect illuminance in the measuring point P_1 , i.e. the illuminance measured by the LMT Digital Illuminance Meter B510, is proportional to the luminous flux of the ELS, and that the error, given by the expressions for ϵ_{pA} , can be neglected. These conclusions are based on the experimental results obtained with *OSRAM* etalons (specifications given in Table 1), and also obvious in results taken from [9, 10] and shown in Table 2. After the determination of the mean value of the integrating parallelepiped (cube) factor, using different etalons *OSRAM*, which are given in Table 1, and which for the control measurements of the luminous flux were done in the Federal Bureau of Measures and Precious Metals (FBM-PM) [13], it is followed that etalons luminous flux could be measured with error less than 1%. Data for etalons luminous flux, given in Table 1 and taken from [13], are considered as accurate. The error ϵ_{pA} given with (24a) is not included.

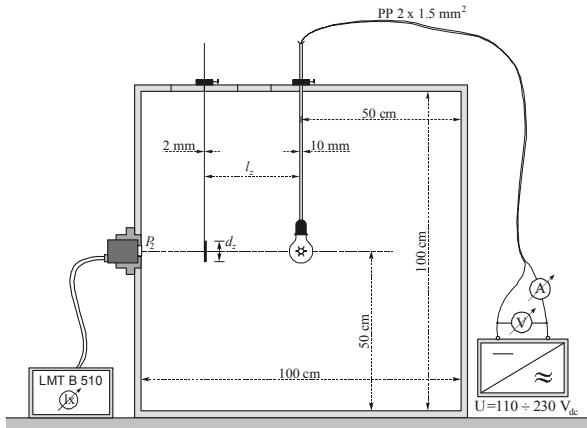


Fig. 7a: The schematic illustration of the luminous fluxmeter system laboratory model with integrating cube.

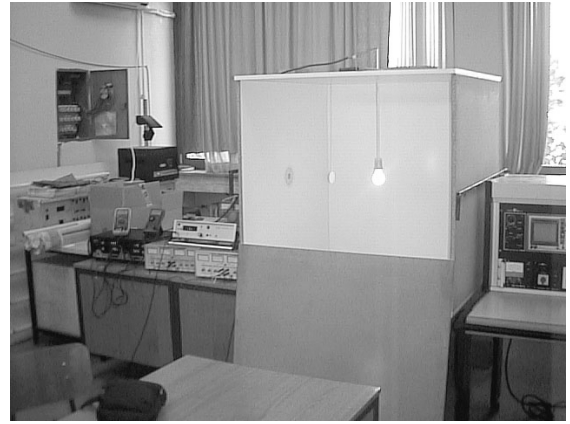


Fig. 7b: The photo of the integrating luminous fluxmeter system laboratory model in, FEE Niš, Lab. of E.I. & I.E.

Theoretical considerations presented in this paper and considerations given in chapter "3.1. Numerical Experiments", theoretically prove hypothesis: Measurement of indirect illuminance in one particular point (center of the one cube's surface) could give high accuracy of the measured results as it is in the case of the sphere geometry.

Table 1: Data of the OSRAM light sources etalons power supply conditions. Luminous flux Φ_0 is given according to [13].

No.	Etalon's Code	P [W]	I [A]	U [V]	Φ_0 [lm]
1.	7/903	25	0.2323	110.0	242.0
2.	8/904	25	0.2318	110.0	237.4
3.	21/129	40	0.3724	110.0	446.4
4.	22/130	40	0.3751	110.0	451.5
5.	73/131	100	0.8941	102.7	1,202.5
6.	27/917	150	1.3845	104.2	1,985.1

Table 2: Experimental determination of the ICF, for two positions of different screens, using the light source etalons and the calculation of the luminous flux of the etalons based on the mean value of ICF as well as on the measured values of the indirect illuminance of the point P_2 vicinity. Colour temperature of all OSRAM etalons was kept constant and according to [13] it is $TCE = 2800$ K.

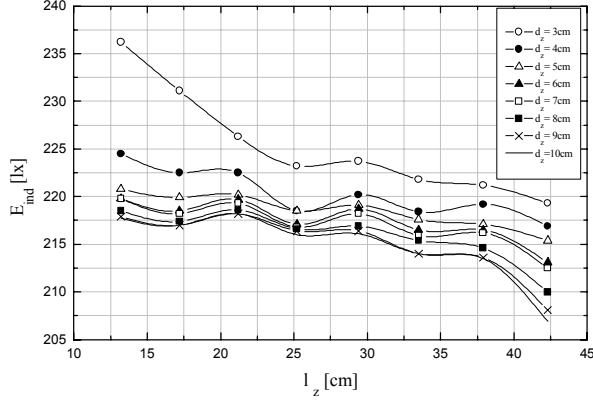
Etalons' data [13]			$d_z = 10$ cm, $l_z = 25$ cm				$d_z = 6$ cm, $l_z = 33.6$ cm			
Code	P [W]	Φ_0 [lm]	$E_{ind pP_1}$ [lx]	C_p^{-1} [lm/lx]	$C_{psr}^{-1} E_{ind pP_1}$ [lm]	$\delta \Phi_0$ [%]	$E_{ind pP_1}$ [lx]	C_p^{-1} [lm/lx]	$C_{psr}^{-1} E_{ind pP_1}$ [lm]	$\delta \Phi_0$ [%]
7/903	25	242.0	215.2	1.1245	240.6	0.593	216.8	1.1162	240.3	0.702
8/904	25	237.4	211.8	1.1209	236.8	0.267	212.9	1.1151	236.0	0.599
21/129	40	446.4	396.0	1.1273	442.7	0.834	401.6	1.1116	445.1	0.283
22/130	40	451.5	403.6	1.1187	451.2	0.072	407.8	1.1072	452.0	0.112
73/131	100	1,202.5	1,087.0	1.1063	1,215.1	1.050	1,095.0	1.0982	1,213.7	0.932
27/917	150	1,985.1	1,789.0	1.1096	1,999.9	0.744	1,801.0	1.1022	1,996.2	0.561
			$C_{psr}^{-1} = 1.117871452$ [lm/lx]				$C_{psr}^{-1} = 1.108403721$ [lm/lx]			

The effects of the screen size and screen position are investigated and assessed on the basis of more than 400 experiments. These experimental results are given in Fig. 8. Presented results show that the screen diameter and screen position are not critical and could be selected in a wide range, depending on the cube and ELS sizes.

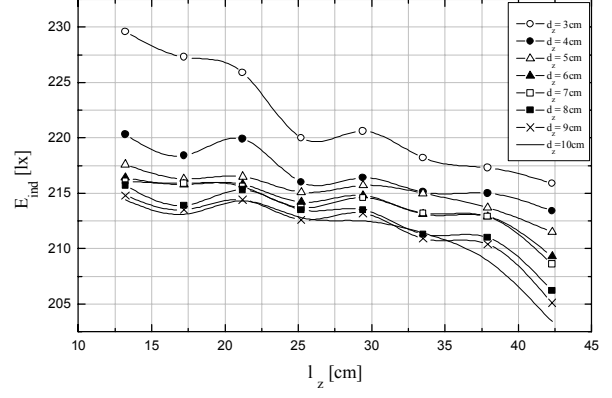
4. CONCLUSION

The mathematical model for Integrating Luminous Fluxmeter System (ILFS) is established in this paper. The model uses System of the Interreflection Equations of the Luminous Flux (SIE-LF), i.e., the Law of luminous flux conservation. The presented analysis uses three following geometries of the Integrating Closed Spaces (ICS): sphere, parallelepiped and cylinder. Interior surfaces of the ICS are ideally diffuse painted, i.e., they form Lambertian surfaces. The so called three-surface model is adopted considering the SIE-LF. Interior of the ICS is illuminated by the ELS with unknown luminous flux.

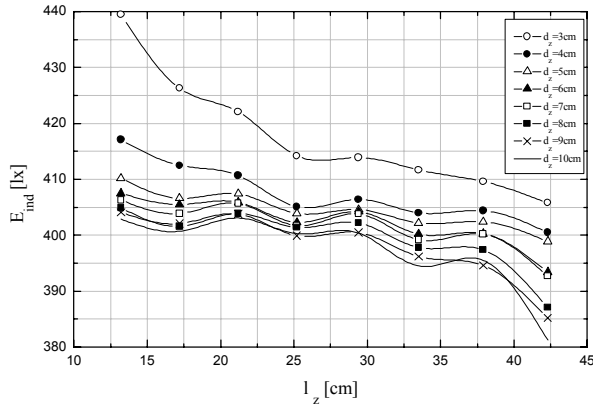
Mean values of the luminous flux distribution on each of three ICS surfaces, as well as mean indirect illuminance of the surface selected for measurement (point P_1 in the center of the of surface S_1), are determined based on the proposed mathematical model. Expression for



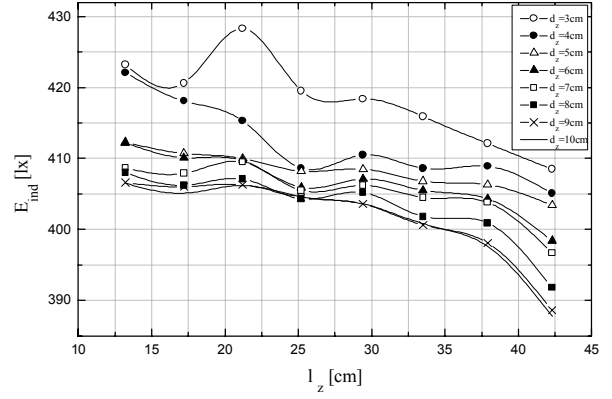
Etalon code: 7/903



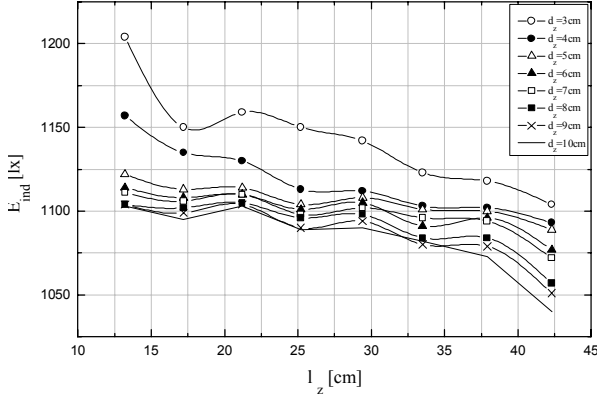
Etalon code: 8/904



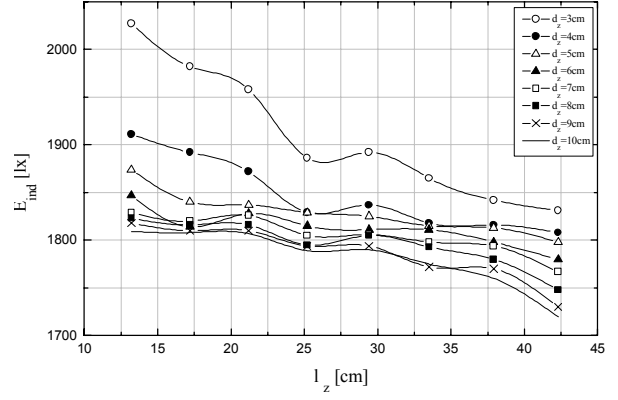
Etalon code: 21/129



Etalon code: 22/130



Etalon code: 73/131



Etalon code: 27/917

Fig. 8: Indirect illuminance measured in point P_1 , $E_{ind} = E_{ind\ pP_1}$, with position of the screen l_z as well as size of the screen d_z as parameters

indirect illuminance calculated for the measuring point P_1 , in this paper is also determined using the SIE-LF. Expression for indirect illuminance in the point P_1 , placed in the center of the surface S_1 , has two terms. The first one is directly proportional to the ESI total unknown luminous flux. The second has significantly smaller influence, and depends on the used geometry, reflectance of the ICS' surfaces and direct luminous flux of the surface S_1 .

Using of different geometries instead of the sphere for the Integrating Luminous Flux Meter System is not new (see for example [4]). Analysis of results presented in this paper suggests that at least theoretically parallelepiped with square bases (close to the cube geometry $a \cong H_p$) and cylinder with circular bases ($3R_c = 2H_c$) can be used as the ICS. The introduced methodical errors are minimal, and can be estimated.

The methodical error is minimized with appropriate selection of the ICS. The numerical results show that for $\rho \geq 0.8$ this error is less than 2.5%. However, with regards to the mathematical model of the sphere shaped ICS, this error is practically zero. The process of the estimation of the total methodical error is illustrated graphically for the two different ELS types, while measuring their unknown radiated luminous flux. Results from the Fig. 6a and Fig. 6b show that error can be even less than 2.5% if ICS' painting has reflectance greater than 0.8, i.e., $\rho > 0.8$.

In the previous published papers [9], [10], the authors presented results of luminous flux measurements related to the laboratory model of the ILFS with cube shaped ICS. Some of these results are used and presented here. The Type A OSRAM etalons are used as the reference ELS. Among the other, following experimental results are highlighted in this paper: results that indicate possibilities for the luminous flux measurement using the cube as the ICS (Table 2), and results showing that size and location of the screen are not critical (Fig. 8).

The proposed mathematical model allows selection of the measuring point P_1 , located on the surface S_1 , in order to minimize methodical calculation error.

Finally, the proposed mathematical model also allows analysis of following ICS geometries: cylinder ICS and cut cone ICS, both with bases that are spherical sectors of the circumscribed sphere. The Equivalent Sphere Method [6]-[8] should be used in such analysis. This research is in progress.

ACKNOWLEDGEMENT: The authors acknowledge support of Prof.Dr.-Ing. Dietrich Gall and LiTG (Deutsche Lichttechnische Gesellschaft) whose help was necessary for presenting the paper. Authors are also grateful to MSTD of the Republic of Serbia.

5. REFERENCES

- [1] А.А.ГЕРШУН: Избранные труды по фотометрии и светлотехнике, Государственное издательство физико-математической литературы, Москва 1958.
- [2] CIE Publication: "The measurement of Luminous Flux", CIE Technical Report, CIE Publ. No. 84, - 1st Edition, 1989.
- [3] IESNA, Ed.: Rea M.S.: Lighting Handbook - Reference & Application, IESNA 8th Edition, New York, 1993, Reprinted 1995.
- [4] G.KRENZKE: "Die Optimierung der Meßanordnung in runden und eckigen Hohlräumen zur Lichtstrombestimmung ausgedehnter Lichtquellen", LICHTTECHNIK, 21. Jahrgang, Nr. 9/1969.
- [5] V.V.MESHOV: Fundamentals of Illumination Engineering, English Trans., Mir Publishers Moscow, Moscow 1981.
- [6] P.D.RANČIĆ: Supplements to the Lighting Engineering Characterizations - Illumination of Closed Spaces, University of Niš, Faculty of Electronic Eng., Niš, 1997. (in Serbian).
- [7] P.D.RANČIĆ: "Characterization of the Sphere Surface Illumination by the Law of Luminous Flux Conservation", Proc. of CIE Sesion'99, Vol. I, Part 1, pp. 225-227, Warsaw, Poland, June, 24-26, 1999.
- [8] P.D.RANČIĆ, and D.G.ZULKIĆ: "Interior Lighting Calculation of Cut Cone Closed Space Using Equivalent Sphere Models", Proc. of the Int. Lighting Congress CIE MIDTERM MEETING ILC, Vol. II, pp. 148-155, Istanbul, September, 6-16, 2001.

- [9] P.D.RANČIĆ, D.D.VUČKOVIĆ: “*Some Experiences in Creation of the Integrating Photometer Systems*”, Proc. of Int. Conf. *LIGT&LIGHTING*’2002, Vol. 1, pp 252-254, Bucharest, November, 28.-30. 2002.
- [10] P.D.RANČIĆ, D.D.VUČKOVIĆ: “*Realization of the Integrating Photometer (Fluxmeter) System Laboratory Model*”, Proc. of IV Symposium of Industrial Electronic, pp. 101-106, Banja Luka, November, 14-15. 2002. (In Serbian)
- [11] S.Ž.DJOKIĆ: *Contribution to the Comparative Characterization of the Interior Lighting Calculation Methods*, M.Sc. thesis, University of Niš, Faculty of Electronic Engineering. Niš, 2001. (in Serbian)
- [12] S.Ž.DJOKIĆ: “*The Moving Optical Center in Lighting Calculations*”, Journal of the IES, Vol. 32, No 1, Winter 2003, pp. 3-13.
- [13] Federal Bureau of Measures and Precious Metals (FBM-PM): “*Data of the control luminous flux measurements of the etalons OSRAM*”, Beograd, July 2002.
- [14] Laboratory for photometry of the lamps factory TESLA Pančevo: “*Data of the luminous flux measurements of light sources*”, Pančevo, July 2002.

Dipl.ing. Dragan D. VUČKOVIĆ; University of Niš, Faculty of Electronic Engineering, Laboratory of Electrical Installation and Illumination Engineering, P.O. Box 74, 18000 Niš, Srbija Tel: +381 18 529305; Fax: +381 18 524 931; E-mail: dvucko@elfak.ni.ac.yu

Prof.dr Predrag D. RANČIĆ; University of Niš, Faculty of Electronic Engineering, Laboratory of Electrical Installation and Illumination Engineering, P.O. Box 74, 18000 Niš, Srbija Tel: +381 18 529305; Fax: +381 18 524 931; E-mail: prancic@elfak.ni.ac.yu
--